Study on the Electromagnetic Flux Generation using the New 2d-axial Capability of Electromagnetism Solver in LS-DYNA

Kunio Takekoshi

Terrabyte Co., Ltd, NOV BLDG 3F, 3-10-7, Yushima, Bunkyo-ku, Tokyo, 113-0034, Japan

1 Introduction

Many scientists are greatly interested in pictures which could be observed under magnetic field over 1000 T. This is because novel phenomena will be expected in this kind of extreme condition like ultra-high pressure environment, ultra-low temperature. In 1000 T condition, cyclotron radius of free electron becomes about fermi wave length, and then it is theoretically predicted that novel quantum state will be revealed.

Historically, it has been reported that the generation of magnetic field over 1000 T was carried out using detonation technique outside laboratory room. However, it is very challenging to precisely measure magnetic state of materials while precisely controlling temperature of the material outside laboratory room.

The Electromagnetic Flux Compression technique is well known for one of the techniques that can generate significant large magnetic field inside laboratory room, and the World's best record by this technique is 730 T achieved by the International Megagauss Science Laboratory, the ISSP, University of Tokyo [1, 2, 3]. It is expected that improving this technique will realize the generation of magnetic field over 1000 T.

However, it is also challenging to improve the method. There are a lot of key factors for the generation of significantly large magnetic field, and scientists are trying a lot of combination of key factors, parameters to obtain the large magnetic field. Since an experiment requires a lot of preparation time and cost, systematic parameter survey cannot be done enough. Thus, numerical simulation technique is needed for the effective parameter survey.

Numerical simulations have been reported using 2D-axisymmetric finite element method [4, 5]. However, these previous studies did not take strain rate effect, thermal effect, and volumetric strain effect into consideration. On the contrary, LS-DYNA is able to consider these effects, thus LS-DYNA will help the development of the experimental system, and will reveal the detail mechanism of dynamical process during the experiment.

Author has reported the simulation results of the Electromagnetic Flux Compression using structural-thermal-electromagnetic coupling technique by LS-DYNA. However, it takes a lot of calculation time (more than 10 days with 28 CPUs) to obtain analysis result. It is desired to reduce calculation time of the simulation of the Electromagnetic Flux Compression. This paper reports the usability of the EM 2D axisymmetric solver in the simulation of the Electromagnetic Flux Compression.

2 The Electromagnetic Flux Compression

Fig.1 and Fig.2 show the main parts of Electromagnetic Flux Compression system developed by the ISSP. The system consists of four coils, the liner, primary, support, and Helmholtz coils. The liner and primary coils are made of copper (or can be represented as a single turn copper coil). The support coil is made of steel (a single turn steel coil). The Helmholtz coil is composed of two coils (242 turns for each coil) using copper wire.

A specimen of interest is placed at the center of the liner coil during experiment with pickup coils to measure magnetic field, and its temperature is usually controlled using a cryostat.

The experimental procedure is as follows;

- 1. The external seed field is developed from 0 to certain value (typically 3.8 T) within 20 milliseconds using the Helmholtz coil. Time history of the electric current injected into the Helmholtz coil is shown in Fig.3, and its direction of the electric current $I_{\mathrm{H.}}$ is depicted in Fig. 1(a). The direction of the seed field $B_{\mathrm{ext.}}$ is also depicted along the coil axis.
- 2. After the achievement of the certain value of the seed magnetic field, the primary and support coils are driven to emerge induced electric current on the surface of the liner coil. The direction of

the electric current $I_{\mathrm{p.}}$ injected into primary and support coils is shown by the arrow depicted in the Fig. 1(a). Here, time history of the injected electric current is shown in Fig.4.

- 3. The liner coil is imploded by the Lorentz repulsion force between the linear and primary coils. The typical period of the implosion of the liner coil is about 40 microseconds.
- 4. The induced current in the liner mainly generates ultra-high magnetic field (several hundred Tesla) in the center of the liner coil. The direction of the ultra-high magnetic field is the same as that of the external seed field.

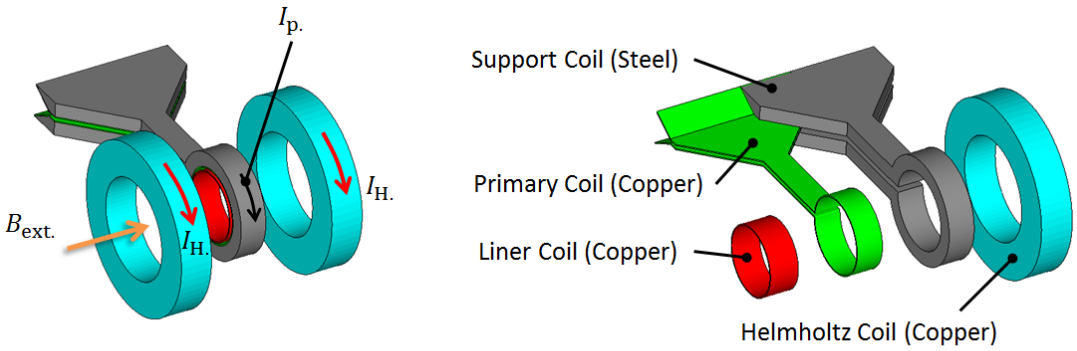

Fig.1: The Electromagnetic Flux Compression developed by the ISSP [1, 2, 3].

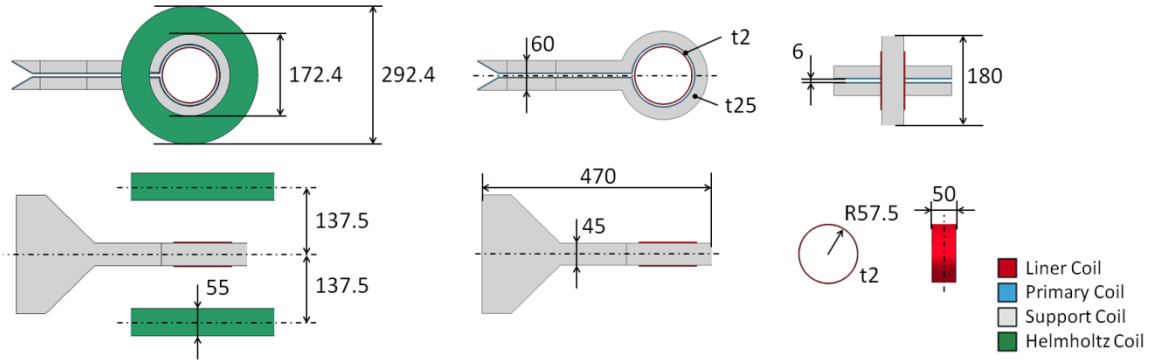

Fig.2: Geometry of a simulation model of the Electromagnetic Flux Compression. The unit in this figure is mm.

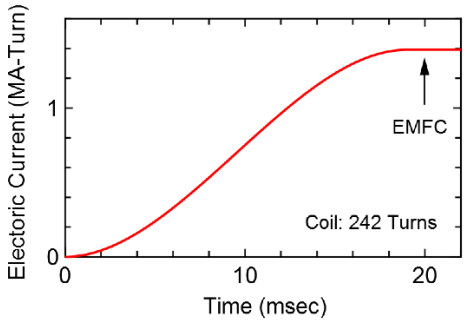

Fig.3: Time history of electric current injected into the Helmholtz coil. The EMFC starts at 20 msec.

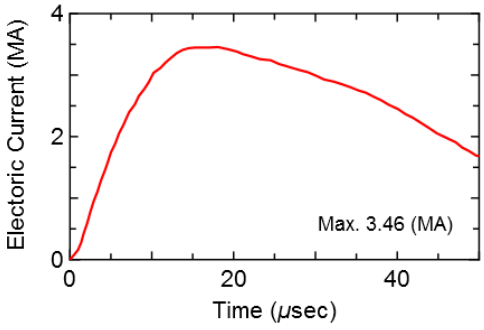

Fig.4: Time history of electric current injected into the primary and support coils [2].

3 Analysis Model

3.1 Overview

Figure 5 shows an analysis model for the 2D-axisymmetric EM solver, one quarter model. The liner, primary, and support coils are modeled in common with the analysis model for the 3D EM solver previously reported [6, 7]. The Helmholtz coil is also modeled, but consists of 16 wires in each coil. The reason for making 16 wires is explained in next. Additionally, a pickup coil is newly modeled for the measurement of magnetic field passing through the pickup coil. Mesh discretization for the liner, primary, and support coils in the EM 2D axisymmetric model is the same as that in the 3D EM model.

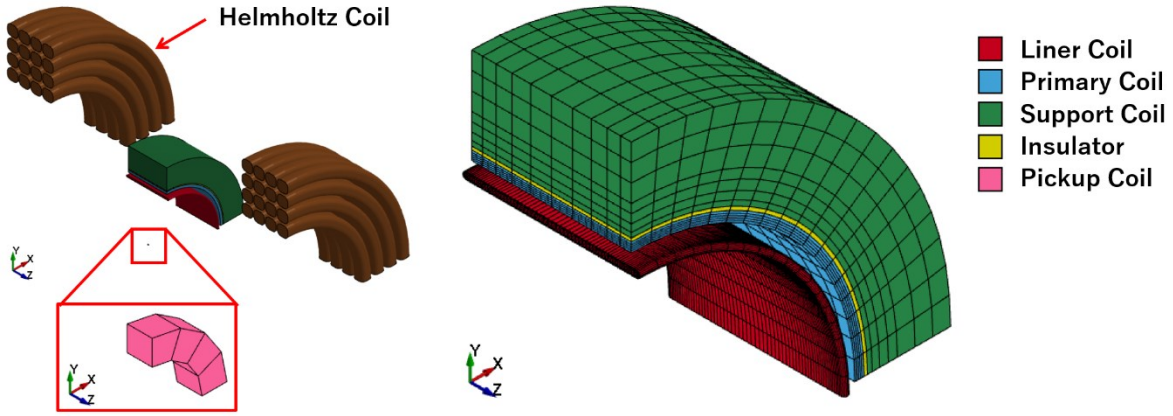

Fig.5: The simulation model for the 2D-axisymmetry EM solver used in this study.

3.2 Boundary Conditions

Boundary conditions applied in the model for the 2D-axisymmetric EM solver are shown in Fig.6. Since the liner, primary, and support coils are modelled as deformation body, boundary conditions for 1/4 model are applied. In addition, 45 degree plane as shown in Fig.6 is also constrained, because the EM-2D axisymmetric solver works on this cross section, and then copies the EM solutions through these parts.

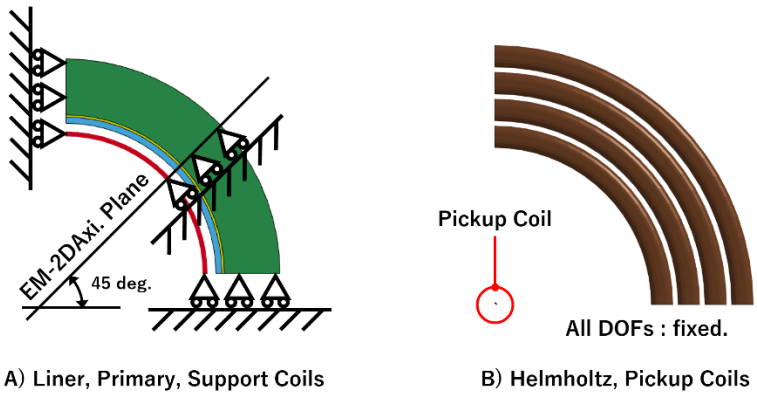

Fig.6: Boundary conditions for the model of the 2D-axisymmetry EM solver used in this study.

3.3 Helmholtz coil

The major difference from an analysis model for the 3D EM solver is that material models **`*EM_MAT_...`** mtype 2 or 4 are only available in the 2D-axisymmetric EM solver. In other words, **`*EM_CIRCUIT_SOURCE`** is not available in the 2D-axisymmetric EM solver for the modelling of winding coils, and it is necessary to model each wire of a coil.

Because of the limitation of unavailability of ***EM_CIRCUIT_SOURCE** in the 2D-axisymmetric EM solver mentioned above, 242 copper wires must be modeled in each coil of the Helmholtz coil. However, instead of modelling 242 copper wires, 16 copper wires with 12.3 mm in width for each wire are modeled in the model for the reduction of modelling cost as shown in Fig 5. Since skin depth of copper material is around 13 mm in the development stage of the external field from 0 to 20 milliseconds (25 Hz), the reduction of coil modelling is acceptable.

3.4 Pickup coil

The second major difference from the analysis model for the 3D EM solver is that ***EM_DATABASE_POINTOUT** is not available for the measurement of magnetic field along with the coil axis which is equivalent to the rotational axis of 2D-axisymmetric solver. Instead of using the keyword, a pickup coil model is modeled to evaluate the magnetic field in 2D-axisymmetric simulation. Similar to experimental techniques, the magnetic field through the center of the pickup coil can be measured from the voltage drop of the coil.

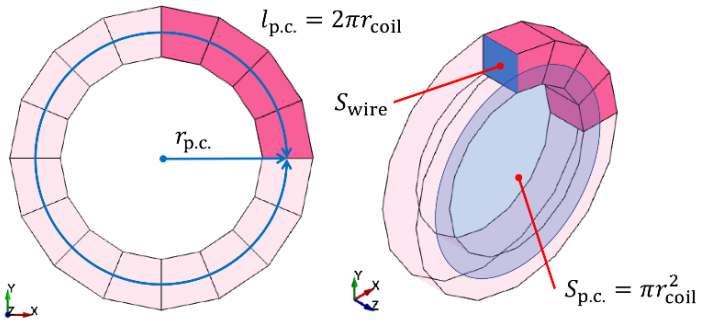

Configuration of pickup coil:
$r_{\text{p.c.}} = 1.0\ (\text{mm})$
$S_{\text{p.c.}} = \pi\ (\text{mm}^2)$
$l_{\text{p.c.}} = 2\pi\ (\text{mm})$
$S_{\text{wire}} = 0.16\ (\text{mm}^2)$

Fig.7: Configuration of the pickup coil used in this study.

Let us consider the pickup coil as shown in Fig.7. The induced current I_{ROGO} in the pickup coil is measured using ***EM_DATABASE_ROGO**, and then the induced voltage drop $V_{\text{p.c.}}$ in the pickup coil can be evaluated using the following formula, Eq. 1.

$$V_{\text{p.c.}}(t) = R_{\text{p.c.}} I_{\text{ROGO}}(t) = \rho \frac{l_{\text{p.c.}}}{S_{\text{wire}}} I_{\text{ROGO}}(t) \tag{1}$$

Here, $R_{\text{p.c.}}$ is the resistivity of the pickup coil, ρ is the electrical resistivity of copper, $l_{\text{p.c.}}$ is the length of coil wire and equals to $2\pi r_{\text{p.c.}}$, S_{wire} is the cross-sectional area of the coil wire.

Since the relationship between the magnetic flux Φ passing through the pickup coil and the induced voltage drop $V_{\text{p.c.}}$ is expressed by Eq. 2,

$$V_{\text{p.c.}}(t) = \frac{d\Phi(t)}{dt} = S_{\text{p.c.}} \frac{dB(t)}{dt} \tag{2}$$

Here, $S_{\text{p.c.}}$ is the effective area of the pickup coil passed by magnetic field.

By considering a relationship between the magnetic flux Φ and the induced voltage drop $V_{\text{p.c.}}(t)$, the magnetic field as a function of time is evaluated using the following formula, Eq. 3. This formula is used in this study to evaluate magnetic field generated by the Electromagnetic Flux Compression technique.

$$B(t) = \frac{1}{S_{\text{p.c.}}} \int_0^t V_{\text{p.c.}}(t')dt' = \int_0^t R_{\text{p.c.}} I_{\text{ROGO}}(t')dt' \tag{3}$$

3.5 Injection of the primary electric current

The electrical current to drive the Electromagnetic Flux Compression in the 2D-axisymetric model is injected into the primary coil unlike the 3D model for the simplicity of the development of the model. The circuit including the primary and support coils is a little bit complex. The electrical potential of these coils is set to the same value at the electric terminal far from the coil part, and path of the electrical current is naturally selected by itself. There is no idea to utilize **`*EM_CIRCUIT_CONNECT`** for the parallel connection of these two coils.

3.6 Material Parameters

The relationship between components, material, and corresponding constitutive model for the mechanical solver is listed in Table 1. The liner and primary coils are subjected to hi-temperature state because of significantly large joule heat effect, and is also subjected to the hi-speed compression state of stress during the generation of magnetic field, **`*MAT_224`** is employed in order to taken temperature dependent Young's modulus as well as stress – strain relationship, and strain rate effect.

Table 1: Components, material, and corresponding constitutive model for the Electromagnetic Flux Compression System in this study.

Component	Material	Constitutive model	EOS	Constants
Liner Coil	Copper	Johnson-Cook [8]	Gruneisen	Ref. [9, 10]
Primary Coil	Copper	Johnson-Cook	Gruneisen	Ref. [9, 10]
Support Coil	Steel	Johnson-Cook	Gruneisen	Ref. [11]
Helmholtz Coil	Copper	Rigid	-	-
Pickup Coil	Copper	Rigid	-	-

Materials for the components and corresponding EOS model of electrical conductivity for the electromagnetism solver used in this study are listed in Table 2.

The electrical property for the liner and primary coils is modelled using the Burgess Model [12] considering temperature and relative volume dependences. The support coil is modelled using tabulated EOS considering electrical conductivity as a function of temperature.

Table 2: Components, material, and corresponding EOS of conductivity in this study.

Component	Material	EOS	Constants
Liner Coil	Copper	Burgess Model [12]	Ref. [12]
Primary Coil	Copper	Burgess Model	Ref. [12]
Support Coil	Steel	Tabulated Data	Ref. [13]
Helmholtz Coil	Copper	-	-
Pickup Coil	Copper	-	Ref. [14]

Material constants used by thermal solver are determined by references [9, 15] for the liner and primary coils (copper), and by references [11, 15] for the support coil (steel). In this study, temperature dependence of thermal conductivity and specific heat are considered using **`*MAT_THERMAL_ISOTROPIC_TD_LC`**.

3.7 Timestep

In this study, time step considered in the thermal, structral, and electromagnetism solvers is fixed or less than 1.0×10^{-8} sec during the Electromagnetic Flux Compression phase.

4 Analysis Results and Discussion

Timestep for the 3D EM model is comparable to CFL condition timestep which varies from 2.8×10^{-9} to 1.3×10^{-8} sec according to the output of **`*EM_DATABASE_TIMESTEP`**. Timestep for the EM 2D-axisymmetric calculation is about ten times less than the CFL condition timestep. The timestep values in 2D and 3D solver are acceptable, and it is difficult to reduce timestep in the 3D calculation, because it takes more than 260 hours with 28 CPUs to obtain the analysis result in the 3D model considered here. On the contrary, it takes 20 hours with 28 CPUs to obtain analysis result in the 2D simulation studied. This drastic reduction of calculation time from 260 hours to 20 hours is the biggest advantage of the EM 2D-Axisymmetric solver.

Figure 8 shows a comparison of generation of magnetic field predicted. The 2D-axisymmetric result successfully traces the 3D result until 40 T in magnetic field. However, the 2D-axisymmetric solver is not able to analyze the model beyond 40 T.

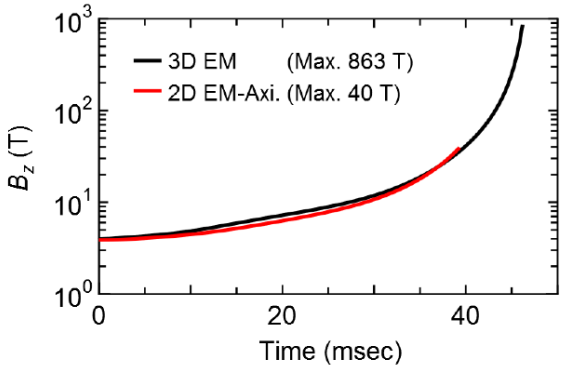

Fig.8: Time history of generation of magnetic field at the center of the coil.

This is because the thermal solver stops the calculation. Figure 9 shows contour plots about temperature distribution at 39 microseconds after the Electromagnetic Flux Compression starts. In the 3D result, the maximum temperature is around 1300 K, below the melting point of copper material. On the other hand, significant high temperature point around 5000 K is observed on the surface of the liner coil in the 2D result. Moreover, the area showing high temperature in the 2D result is different from that in the 3D result. Thermal properties are not ready for more than 5000 K which had been prepared by extrapolating from the melting point to 5000 K.

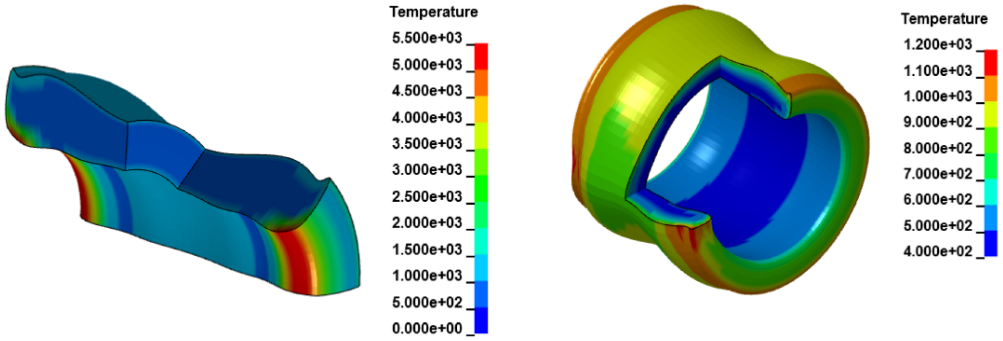

Fig.9: Contour plots of temperature for the liner coil at 39 microseconds after the Electromagnetic Flux Compression starts.

From the experimental view point, the liner coil is subjected to high temperature due to significant large joule heating, and then the liner coil is melted and vapored after the experiment. Thus, there is no remnants of the liner coil. This is why the high temperature observed in the 2D result might be acceptable. However, the reason for the difference of temperature distribution is not given yet.

One of the reasons to explain the difference of temperature distribution is deformation of the liner coil. The primary and support coils are approximately considered as a single ring coil, but there is a gap or in other words disconnection of the ring as shown in Fig. 1. This gap disturbances magnetic field, and then the shape of the liner coil is affected. Indeed, the shape of the liner coil during the Electromagnetic Flux Compression cannot be considered axisymmetric as shown in Fig. 10. Induced current flow pattern on the liner coil must be depend on the surface shape of the liner coil as well as magnetic field, and then temperature distribution will be affected. Also, these effects should affect coil impedances.

Historically, a feed gap compensator [2] was proposed to reduce the gap effect. In future, it is possible to incorporate the feed gap compensator into the experimental system for the stability of generation of magnetic field beyond 1000 T. Therefore, the Electromagnetic Flux Compression system

studied here plus the feed gap compensator will be successfully simulated using EM 2D axisymmetric solver, and the EM 2D axisymmetric solver will give us the essentially same result as the EM 3D result.

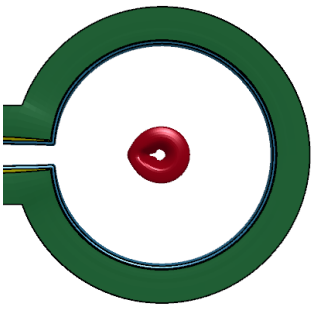

Fig.10: Deformation of the liner coil (red part) predicted by 3D EM solver.

5 Conclusion

This report presents usability of the EM 2D axisymmetric solver in the simulation of the Electromagnetic Flux Compression technique. The solver gives us the same result until 40 T in the generation of magnetic field, while also gives different temperature distribution from the 3D result. This difference is discussed. The major advantage “saving calculation time” of the EM 2D axisymmetric solver is confirmed.

6 Acknowledgement

The author thanks for helpful support by Dr. Pierre L’Eplattenier and Dr. Inaki Caldichoury, LSTC. The author also thanks for helpful discussion with Professor Shojiro Takeyama and Dr. Daisuke Nakamura, and Dr. Akihiko Ikeda, UTokyo International MegaGauss Science Laboratory. They provided experimental results and showed detailed setup of their experimental apparatus.

7 Literature

[1] Takeyama, S. and Kojima, E., "A copper lined magnet coil with maximum field of 700 T for electromagnetic flux compression," *Journal of Physics D: Applied Physics,* vol. 44, p. 425003, 2011.

[2] Takeyama, S., "The World Highest Magnetic Field as Indoor Generation and Its Application to Solid State Physics," *The Physical Society of Japan,* vol. 67, no. 3, p. 170, 2012.

[3] Takeyama, S., Sawabe, H., and Kojima, E., "Recent Developments of the Electro-Magnetic Flux Compression," *Journal of Low Temperature Physics,* vol. 159, pp. 328-331, 2010.

[4] Miura, N., and Chikazumi, S., "Computer Simulation of Megagauss Field Generation by Electromagnetic Flux-Compression," *Japanese Journal of Applied Physics,* vol. 18, no. 3, p. 553, 1979.

[5] Nakamura, D., Sawabe, H., Matsuda, Y. H. and Takeyama, S., "Dynamical Process of Liner Implosion in the Electromagnetic Flux Compression for Ultra-high Magnetic Fields," *arXiv,* p. 1309.1038, 2013.

[6] Takekoshi, K., "Simulation of the Electromagnetic Flux Compression using LS-DYNA Multi-Physics Capability," *Proceedings of the 10th European LS-DYNA Conference 2015,* 2015.

[7] Takekoshi, K., "Study on Ultra-high Electro-Magnetic Flux Generation using LS-DYNA Multi-Physics Capability," *Proceedings of 14th LS-DYNA Users Meeting & Conference,* 2016.

[8] G. R. Johnson and W. H. Cook, "A constitutive model and data for metals subjected to large strains, high strain rates and high temperatures.," *Proc. 7th Int. Symposium on Ballistics.,* pp. 541-547, 1983.

[9] B. Banerjee, "An evaluation of plastic flow stress models for the simulation of high-temperature and high-strain-rate deformation of metals," *cond-mat,* p. 0512466v1, 2005.

[10] H. M. Ledbetter and E. R. Naimon, "Elastic Properties of Metals and Alloys. II. Copper," *J. Phys. Chem. Ref. Data,* vol. 3, no. 4, pp. 897-935, 1974.

[11] B. Banerjee, “The Mechanical Threshold Stress model for various tempers of AISI 4340 steel,” *cond-mat,* p. 0510330v1, 2005.
[12] T. J. Burgess, "Electrical resistivity model of metals," *4th International Conference on Megagauss Magnetic-Field Generation and Related Topics, Santa Fe, NM, USA,* 1986.
[13] Japan Society of Thermophysical Properties, Thermophysical Properties Handbook, YOKENDO, 2008, p. 210.
[14] R. A. Matula, "Electrical Resistivity of Copper, Gold, Palladium, and Silver," *J. Phys. Chem. Ref. Data,* vol. 8, no. 4, p. 1147, 1979.
[15] R. W. Powel, C. Y. Ho and P. E. Liley, "Thermal Conductivity of Selected Materials," *National Standard Reference Data Series - National Bureau of Standards - 8,* 1966.